Atmos. Chem. Phys., 24, 13587–13601, 2024
https://doi.org/10.5194/acp-24-13587-2024

Atmospheric Chemistry and Physics
Open Access
EGU

Research article

The variations in volatile organic compounds based on the policy change for Omicron in the traffic hub of Zhengzhou

Bowen Zhang[1,3,★], Dong Zhang[2,3,★], Zhe Dong[2,3], Xinshuai Song[1,3], Ruiqin Zhang[1,3], and Xiao Li[1,3]

[1]School of Ecology and Environment, Zhengzhou University, Zhengzhou 450001, China
[2]College of Chemistry, Zhengzhou University, Zhengzhou 450001, China
[3]Institute of Environmental Sciences, Zhengzhou University, Zhengzhou 450001, China
★These authors contributed equally to this work.

Correspondence: Xiao Li (lixiao9060@zzu.edu.cn)

Received: 27 February 2024 – Discussion started: 8 March 2024
Revised: 2 October 2024 – Accepted: 15 October 2024 – Published: 10 December 2024

Abstract. Online volatile organic compounds (VOCs) were monitored before and after the Omicron policy change at an urban site in polluted Zhengzhou from 1 December 2022 to 31 January 2023. The characteristics and sources of VOCs were investigated. The daily mean concentrations of $PM_{2.5}$ and total VOCs (TVOCs) ranged from 53.5 to 239.4 $\mu g\,m^{-3}$ and 15.6 to 57.1 ppbv, respectively, with mean values of $111.5 \pm 45.1\ \mu g\,m^{-3}$ and 36.1 ± 21.0 ppbv, respectively, throughout the period. Two severe pollution events (designated as case 1 and case 2) were identified in accordance with the National Ambient Air Quality Standards (NAAQS) (China's National Ambient Air Quality Standards (NAAQS) from 2012). Case 1 (5 to 10 December $PM_{2.5}$ daily mean $= 142.5\ \mu g\,m^{-3}$) and case 2 (1 to 8 January $PM_{2.5}$ daily mean $= 181.5\ \mu g\,m^{-3}$) occurred during the infection period (when the policy of "full nucleic acid screening measures" was in effect) and the recovery period (after the policy was canceled), respectively. The $PM_{2.5}$ and TVOC values for case 2 are, respectively, 1.3 and 1.8 times higher than those for case 1. The precise influence of disparate meteorological circumstances on the two pollution incidents is not addressed in this study. The results of the positive matrix factor modeling demonstrated that the primary source of VOCs during the observation period was industrial emissions, which constituted 32 % of the total VOCs, followed by vehicle emissions (27 %) and combustion (21 %). In case 1, industrial emissions constituted the primary source of VOCs, accounting for 32 % of the total VOCs. In contrast, in case 2, the contribution of vehicular emission sources increased to 33 % and became the primary source of VOCs. The secondary organic aerosol formation potential for case 1 and case 2 were found to be 37.6 and 65.6 $\mu g\,m^{-3}$, respectively. In case 1, the largest contribution of SOA formation potential (SOAP) from industrial sources accounted for the majority (63 %; 23.8 $\mu g\,m^{-3}$), followed by vehicular sources (18 %). After the end of the epidemic and the resumption of productive activities in the society, the difference in the proportion of secondary organic aerosol (SOA) generated from various sources decreased. Most of the SOAP came from solvent use and fuel evaporation sources, accounting for 32 % (20.9 $\mu g\,m^{-3}$) and 26 % (16.8 $\mu g\,m^{-3}$), respectively. On days with minimal pollution, industrial sources and solvent use remain the main contributors to SOA formation. Therefore, the regulation of emissions from industry, solvent-using industries, and motor vehicles needs to be prioritized to control the $PM_{2.5}$ pollution problem.

Published by Copernicus Publications on behalf of the European Geosciences Union.

1 Introduction

Volatile organic compounds (VOCs) in the atmosphere have high reactivity and can react with nitrogen oxides (NO_x) to form a series of secondary pollutants such as ozone (O_3) and secondary organic aerosol (SOA), resulting in regional air pollution (Li et al., 2019; Hui et al., 2020). The problem of O_3 pollution has been plaguing major urban agglomerations in China (Zheng et al., 2010; Li et al., 2014; Wang et al., 2017). SOA is an important component of fine particulate matter ($PM_{2.5}$) and contributes significantly to haze pollution (Liu et al., 2019). $PM_{2.5}$ remains the most significant air pollutant in many Chinese cities for years (Shao et al., 2016; Wu et al., 2016). In addition, VOCs, represented by the benzene homologues, can cause damage to the kidneys, liver, and nervous system of humans when they enter the body (Zhang et al., 2018).

Studies have shown that the most common VOC components in China are alkanes, olefins, aromatic hydrocarbons, oxygenated VOCs (OVOCs), and halogenated hydrocarbons, among which alkanes are the most abundant species (Liu et al., 2020; C. Zhang et al., 2021). VOCs in the atmosphere have a wide range of sources, and VOCs in different regions are affected by multiple factors such as local geography, climate, and human activities (Mu et al., 2023; Zou et al., 2023). The above reasons lead to significant regional and seasonal differences in the characteristics of VOCs (Song et al., 2021). For example, the annual average concentration of VOCs in the coastal background area of the Pearl River Delta is 9.3 ppbv. The seasonal variation trend of VOCs is high in autumn and winter and low in summer (Yun et al., 2021). In contrast, the average VOC concentration in autumn and winter in Beijing was 22.6 ± 12.6 ppbv, and the VOC concentration in the winter heating period was twice that in the autumn non-heating period (Niu et al., 2022).

Moreover, the sources of VOC components in different regions are also related to the local industrial structure and living habits. In rural areas of the North China Plain in winter, it is found that the SOA formation potential (SOAP) of VOCs under low-NO_x conditions is significantly higher than that under high-NO_x conditions, and the increase in aromatic hydrocarbon emissions caused by coal combustion is the main reason for the higher SOAP in winter (Zhang et al., 2020). Li et al. (2022) found that the average increased concentration of acetylene was 4.8 times from autumn to winter in the Guanzhong Plain, indicating that fuel combustion during the heating period in winter has a significant impact on the composition of VOCs. In contrast, continuous observations conducted by Zhou et al. (2022) in the suburbs of Dongguan in summer found that industrial solvent usage, liquefied petroleum gas (LPG), and oil and gas volatilization were the main sources of VOCs. The results highlighted a wide variation in characteristics, sources and chemical reactions of VOCs in the atmosphere; thus it is necessary to investigate VOCs in different cities when formulating control measures.

Zhengzhou, as the capital of Henan Province, is an important transportation hub and economic center in the Central Plain region. Zhengzhou is currently facing significant air pollution problems, with the air quality index at the bottom of the national ranking of 168 cities for many years. In January 2023, for example, the number of polluted days with $PM_{2.5}$ as the primary pollutant was 17, and the daily average value of $PM_{2.5}$ reached a maximum of 298 $\mu g\,m^{-3}$ (https://www.aqistudy.cn/historydata/daydata.php?city=%E9%83%91%E5%B7%9E&month=202301, last access: January 2024), which is almost 300 % higher than the Chinese daily average standard (Class II; 75 $\mu g\,m^{-3}$). The studies of VOCs were carried out in Zhengzhou in recent years, which focused on the characteristics and sources of VOCs during pollution episodes (Lai et al., 2024) or before the COVID-19 outbreak (Li et al., 2020; D. Zhang et al., 2021). While some atmospheric VOCs studies involving the impact of the COVID-19 lockdown have been performed in India (Singh et al., 2023a) and in China (e.g., Pei et al., 2022; Jensen et al., 2021; Zuo et al., 2024), or with respect to toluene, benzene, *m*/*p*-xylene, and ethylbenzene only (e.g., Sahu et al., 2022; Singh et al., 2023b), a gap persisted in the investigation of VOCs due to the impact of the abolishment of China's zero-COVID policy. Furthermore, some studies have discussed the impact of changes in human production activities on air pollution during and after the outbreak of COVID-19 (e.g., Ma et al., 2022; Jiang et al., 2023; Song et al., 2023), but as mentioned earlier, there are only a few studies with an in-depth exploration of the changes in VOCs and none dealing with ending the zero-COVID policy during the Omicron variant infection period.

In this study, we conducted continuous online observations of VOCs during the polluted winter season at an urban site in Zhengzhou. The study covered the period following the removal of lockdown measures. We focused on pollution events when the daily average $PM_{2.5}$ concentration exceeded 75 $\mu g\,m^{-3}$ (China's Class II standard) for more than 3 consecutive days. Days with $PM_{2.5}$ concentrations below 35 $\mu g\,m^{-3}$ (China's Class I standard) were classified as clean days. During this period, China lifted the zero-COVID strategies, announcing the 10 measures for optimizing COVID-19 rules on 7 December 2022 (http://www.news.cn/politics/2022-12/07/c_1129189285.htm, last access: January 2024). Zhengzhou's epidemic prevention and control measures changed with the issuance of Circular No. 163 on 4 December 2022, which allowed the reopening of closed public places. As a result, movement within Zhengzhou increased, and social production resumed. Our research specifically examines the period dominated by the COVID-19 Omicron variant, which demonstrates notable differences from the early virus strains (i.e., original SARS-CoV-2 virus and Delta) in terms of geographical transmission, the scale of the infected population, and symptom manifestation (Petersen et al., 2022; Merino et al., 2023).

After the quarantine policy was lifted, people basically rested at home due to infection or fear of infection with Omicron. The resumption of normal production and life depends on herd immunization. This outbreak event is the longest in duration and the largest in number of infections since the 2020 outbreak of the Novel Coronavirus in Zhengzhou. It would be beneficial to investigate the impact of this event on emissions related to transportation and industrial production. This change is worth exploring in terms of its impact on transportation and industrial production emissions. Therefore, the characteristics of and variations in VOCs during different periods were investigated to assess their impact on the formation of SOA and to provide scientific insights for developing future pollution control policies in Zhengzhou.

2 Materials and methods

2.1 Sample collection and chemical analysis

The online VOC observation station is located on the roof of the Zhengzhou Environmental Protection Monitoring Center, which is in an urban area. The sampling site is close to main roads on three sides (150 m away from Funiu Road on the east side, 200 m away from Qinling Road on the west side, and connected to Zhongyuan Road on the south side) and surrounded by residential areas and commercial areas without other large nearby stationary sources. The sampling period for this study was from 1 December 2022 to 31 January 2023, and serious $PM_{2.5}$ pollution in Zhengzhou was of frequent occurrence during December and January (https://www.aqistudy.cn/historydata/monthdata.php?city=%e9%83%91%e5%b7%9e#:~:text=%E7%94%9F%E5%91%BD%E6%9D%A5%E6%BA%90%E8%87%AA%E7%84%B6%EF%BC%8C%E5%81%A5, last access: 14 July 2024). Apart from a brief occurrence of rain and snow on 25 December, the sampling days were either sunny or cloudy. The wind speed (WS), temperature (Temp), and relative humidity (RH) during this period were $1.3 \pm 0.9\ m\ s^{-1}$, $5.3 \pm 3.2\ °C$, and $38.9 \pm 19.0\ \%$), respectively, similar to the values observed in previous years in Zhengzhou. It is interesting to point out that the sampling period in the present study covered the entire infection period of Omicron in Zhengzhou, including the phase of the surge in the infected population (infection period from 1 to 31 December 2022) and the phase of the restoration of production and livelihood (recovery period from 1 to 31 January 2023 in 2023) (Fig. S1 in the Supplement; CCDCP, 2023).

The VOCs were measured hourly using a gas chromatography flame ionization detector/mass spectrometry (GC-FID/MS) (TH-PKU 300B, Wuhan Tianhong Instrument Co., Ltd., China). The TH-PKU 300B instrument includes an electronic refrigeration ultra-low temperature preconcentration sampling system, an analysis system, and system control software. The ambient VOCs in the first 5 min of each hour were collected by the sampling system and then entered the concentration system. Under low-temperature conditions, the VOC samples collected were frozen in the capillary capture column and then quickly heated and resolved so that the compounds entered the analysis system. After separation by the chromatographic column, the compounds were monitored by FID and MS detectors. During the detection process, the atmospheric samples collected undergo analysis through two distinct pathways. C_2–C_5 hydrocarbons are analyzed using FID, while C_5–C_{12} hydrocarbons, halocarbons, and OVOCs are analyzed with a MS detector. After excluding species with missing data exceeding 10 %, the detected volatile organic compounds include 29 alkanes, 11 alkenes, 17 aromatics, 35 halocarbons, 12 OVOCs, 1 alkyne (acetylene), and 1 sulfide (CS_2), with a total of 106 compounds. A detailed description of the instrumentation can be found in our previous study (D. Zhang et al., 2021; Shi et al., 2022; Zhang et al., 2024).

The instrument was calibrated every week to ensure the accuracy of VOCs by injecting standard gases with a five-point calibration curve. The detection limit of C_2–C_5 hydrocarbons ranges from 0.007 to 0.099 ppbv; other hydrocarbons range from 0.004–0.045 ppbv, halogenated hydrocarbons range from 0.009–0.099 ppbv, and OVOCs and other compounds range from 0.006–0.095 ppbv. In total, 32 of the monitored VOCs had over 90 % observed data greater than the detection limit, and 34 had more than 50 % observed data greater than the detection limit.

Simultaneous observations at the same site were also carried out for particulate matter ($PM_{2.5}$ and PM_{10}), other trace gases (carbon monoxide (CO), O_3, nitric oxide (NO), and nitrogen dioxide (NO_2)), and meteorological data (Temp, RH, WS, and wind direction (WD)), based on 1 h resolution.

2.2 Positive matrix factorization (PMF) model

The U.S. Environmental Protection Agency (EPA) PMF5.0 model was used for the quantitative source analysis of VOCs (Norris et al., 2014). The principles and methods have been described in detail in previous studies (Mozaffar et al., 2020; D. Zhang et al., 2021). The decomposition of the positive matrix factorization (PMF) mass balance equations is simplified as follows (Norris et al., 2014):

$$x_{ij} = \sum_{k=1}^{p} g_{ik} f_{kj} + e_{ij}, \quad (1)$$

where x_{ij} is the mass concentration of species j measured in sample i; g_{ik} is the contribution of factor k to the sample i; f_{kj} represents the content of the jth species in factor k; e_{ij} is the residual of species j in sample i; p represents the number of factors. The fitting objective of the PMF model is to minimize the function Q to obtain the factor contributions and contours. The formula for Q is given in Eq. (2):

$$Q = \sum_{i=1}^{n}\sum_{j=1}^{m}\left[\frac{x_{ij} - \sum_{k=1}^{p} g_{ik} f_{kj}}{u_{ij}}\right]^2, \quad (2)$$

where n and m denote the number of samples and VOC species, respectively.

Concentrations and uncertainty data are required for the PMF model. In this study, the median concentration of a given species is used to replace missing values with an uncertainty of 4 times of the median values; data that were less than the method detection limit (MDL) were replaced with half the MDL, with an uncertainty of five-sixths of the MDL; and the uncertainty for values greater than the MDL was calculated using Eq. (3). In Eq. (3), EF is the error fraction, expressed as the precision of the VOC species, and the setting range can be adjusted from 5 % to 20 %, according to the concentration difference (Buzcu and Fraser, 2006; Song et al., 2007). c_{ij} is the concentration of species j in sample i, as follows:

$$U_{ij} = \sqrt{(\mathrm{EF} \times c_{ij})^2 + (0.5 \times \mathrm{MDL})^2}. \quad (3)$$

When the concentration of VOCs in the species is less than the value of the detection limit, U_{ij} is calculated using Eq. (4), as follows:

$$U_{ij} = \left(\frac{5}{6}\right)\mathrm{MDL}. \quad (4)$$

VOC species and concentration input into PMF were carefully selected to ensure the accuracy of the PMF results. Species were excluded when over 25 % of the samples were missing or concentration values were below the MDL (Gao et al., 2018); VOCs with a short lifetime in the atmosphere were also excluded unless they are source-relative species (Zhang et al., 2014; Shao et al., 2016). After that, retained VOC species were categorized according to the signal-to-noise ratio (S/N), with $S/N < 0.2$ species categorized as bad, $0.2 < S/N < 2$ species categorized as weak, and $S/N > 2$ species categorized as strong (Shao et al., 2016).

We used a displacement (DISP) of factor elements to assess the PMF modeling uncertainty (for a description, see Paatero et al., 2014). Q was less than 1 %, and no swaps occurred for the smallest $\mathrm{d}Q^{\max}$ in DISP. F_{peak} values from −2 to 2 were tested to explore the rotational stability of the solutions. $Q_{\mathrm{true}}/Q_{\mathrm{exp}}$ is lowest when $F_{\mathrm{peak}} = 0$, so we chose the PMF results for that case (Fig. S2a). After examining 3–8 factors, 20 base runs with 5 factors eventually selected to represent final result. We provide an explanation of the factor selection in the Supplement. Figure S2b includes $Q_{\mathrm{true}}/Q_{\mathrm{exp}}$ and $Q_{\mathrm{robust}}/Q_{\mathrm{exp}}$ for factors three to eight. The slopes of these two ratios changed at five factors, and we found that five factors were more realistic after repeated comparisons of the results at four, five, and six factors.

2.3 SOA generation potential

The contributions of VOC species to SOAP were calculated based on the toluene-weighted mass contribution (TMC) method (Derwent et al., 2010). The methodology for calculating SOAP is as follows:

$$\mathrm{SOAPF}_i = \frac{\text{VOC component } i \text{ to SOA mass concentration increments}}{\text{toluene to SOA mass concentration increment}} \times 100. \quad (5)$$

SOAPF_i is for each VOC is taken from the literature (Derwent et al., 2010). The SOAP value was estimated by multiplying the SOAPF_i value by the concentration of individual VOC species. The SOAP calculations through each VOC are as follows:

$$\mathrm{SOAP} = \sum E_i \times \mathrm{SOAPF}_i. \quad (6)$$

E_i is the concentration of species i.

3 Results and discussion

3.1 Overview of variation in pollutants and meteorological parameters

Figure 1 shows the time series of meteorological parameters, total VOCs (TVOCs), O_3, NO_x, SO_2, CO, and $PM_{2.5}$ during the observed periods. Low WS and Temp were found, with an average value of $1.3 \pm 0.6\,\mathrm{m\,s^{-1}}$ and $5.0 \pm 2.5\,^{\circ}\mathrm{C}$, respectively, during the entire period, comparable with observations at the same site in 2021 (Lai et al., 2024). A total of 62 d of valid data was acquired, with the daily average concentration of $PM_{2.5}$ ranging from 53 to $239\,\mu\mathrm{g\,m^{-3}}$, with the average value of $111 \pm 45\,\mu\mathrm{g\,m^{-3}}$. The concentration of TVOCs ranged from 15.6 to 57.1 ppbv, with an average of 36.1 ± 21.0 ppbv, which is higher than the same period in the previous year (27.9 ± 12.7 ppbv; Lai et al., 2024). During the observation period, the average values of Temp, WS, and RH were $5.0 \pm 2.5\,^{\circ}\mathrm{C}$, $1.3 \pm 0.6\,\mathrm{m\,s^{-1}}$, and 38.9 ± 16.7 %, respectively.

Previous studies have shown that meteorological factors such as low WS, high RH, and low precipitation are responsible for the increase in $PM_{2.5}$ pollution in Zhengzhou in winter (Duan et al., 2019). Our analysis of the correlation between different pollutants and meteorological conditions during the pollution period showed that $PM_{2.5}$, TVOCs, and NO_x were positively correlated with relative humidity (Fig. S3), which is consistent with the results of some previous studies (Wang et al., 2019). The comparisons of the average concentrations of different periods between different periods are presented in Tables 1 and 2. In this study, the WS on clean days ($1.4 \pm 0.8\,\mathrm{m\,s^{-1}}$) was higher than in case 1 ($1.2 \pm 0.9\,\mathrm{m\,s^{-1}}$) and case 2 ($0.9 \pm 0.7\,\mathrm{m\,s^{-1}}$), while the RH was lower by 26.2 % and 12.5 % compared to case 1 and case 2, respectively. These findings indicate that high RH and low WS significantly influence the occurrence of

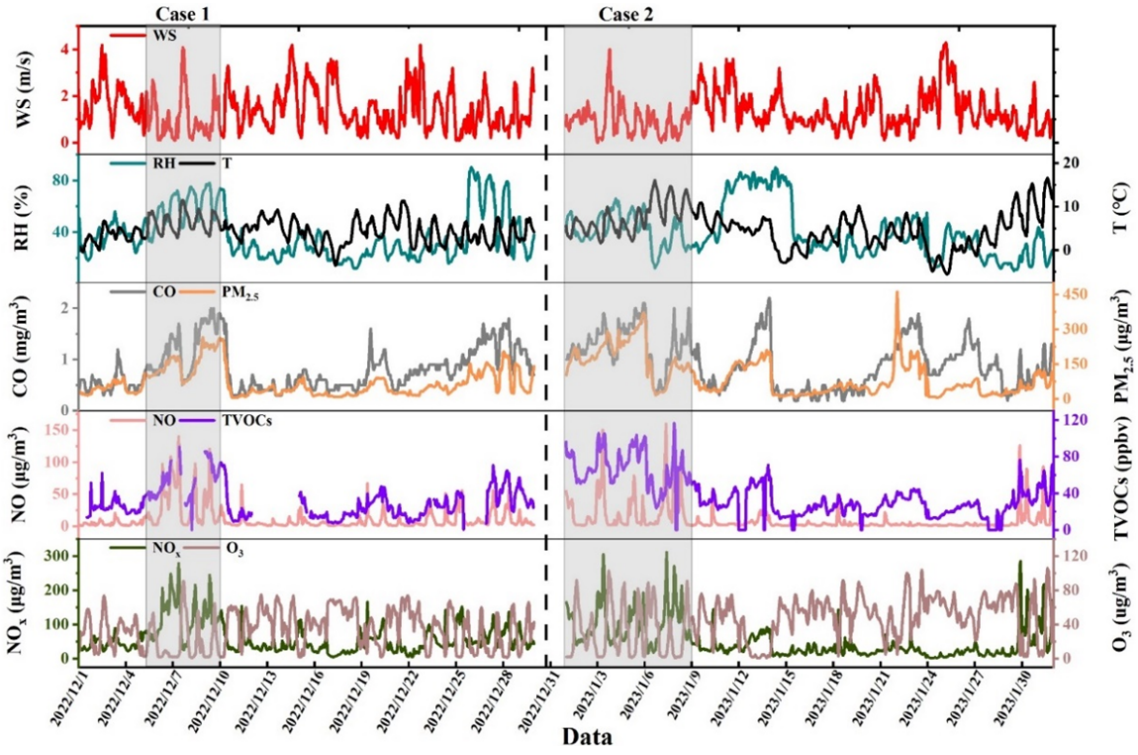

Figure 1. Time series of WS, Temp, RH, CO, $PM_{2.5}$, NO, TVOCs, NO_x, and O_3 during the observation period.

Table 1. The average concentrations of meteorological parameters and pollutants during different processes.

Category	Entire process (1 December 2022–31 January 2023)	Infection period (1–31 December 2022)	Recovery period (1–31 January 2023)	Case 1 (5–10 December 2022)	Case 2 (1–8 January 2023)	Clean days
	$N = 62$ d	$N = 31$ d	$N = 31$ d	$N = 6$ d	$N = 8$ d	$N = 8$ d
WS ($m\,s^{-1}$)	1.3 ± 0.6	1.4 ± 0.6	1.3 ± 0.6	1.2 ± 0.9	0.9 ± 0.7	1.4 ± 0.8
Temp (°)	5.0 ± 2.5	4.7 ± 1.7	5.4 ± 3.1	6.1 ± 2.2	7.4 ± 3.5	4.1 ± 3.0
RH (%)	38.9 ± 16.7	37.6 ± 15.5	40.2 ± 18.2	55.7 ± 14.7	42.0 ± 12.1	29.5 ± 18.1
TVOCs (ppbv)	36.1 ± 21.0	31.9 ± 18.1	39.8 ± 22.4	37.6 ± 27.0	68.2 ± 19.6	22.7 ± 11.1
SO_2 ($\mu g\,m^{-3}$)	11.4 ± 2.7	10.2 ± 2.8	12.7 ± 2.3	11.0 ± 3.7	16.2 ± 6.1	6.5 ± 2.5
NO_2 ($\mu g\,m^{-3}$)	47.2 ± 10.0	46.8 ± 8.6	47.8 ± 11.7	62.7 ± 20.5	65.0 ± 21.3	20.8 ± 15.9
CO ($mg\,m^{-3}$)	0.9 ± 0.2	0.8 ± 0.2	1.1 ± 0.2	1.2 ± 0.5	1.3 ± 0.4	0.5 ± 0.2
O_3 ($\mu g\,m^{-3}$)	34.9 ± 6.0	31.1 ± 4.5	39.0 ± 4.6	21.8 ± 23.7	32.5 ± 29.6	52.6 ± 18.4
$PM_{2.5}$ ($\mu g\,m^{-3}$)	111.5 ± 45.1	86.6 ± 34.6	138.3 ± 39.6	142.5 ± 67.4	181.5 ± 82.7	23.8 ± 16.8

pollution during the observation period. WS, Temp, and RH conditions during infection and recovery periods were generally similar, and meteorology may also have played a role in the differences between pollution events, but its specific influence was not determined here. The average concentration of $PM_{2.5}$ during the recovery period was 1.6 times the value during the infection period. Furthermore, the concentrations of other pollutants, including SO_2, NO_2, CO, and O_3 all showed a similar trend between the infection and recovery periods. The TVOC concentration during the recovery period was 1.2 times the value during the infection period, showing an obviously increasing trend after resuming production. Decreased trends of air pollutants were found in other studies before and after the outbreak of the Novel Coronavirus (COVID-19) in early 2020 (Qi et al., 2021; Wang et al., 2021).

The shaded section in Fig. 1 represents two haze pollution events during the monitoring period. A pollution event is determined when the daily average concentration of $PM_{2.5}$ exceeds $75\,\mu g\,m^{-3}$ (China's Class II standard) for at least 3 consecutive days. Case 1 (5 to 10 December, with daily average $PM_{2.5} = 142.5\,\mu g\,m^{-3}$) and case 2 (1 to 8 January,

Table 2. Concentration of VOC species during different processes (ppbv).

Category	Entire process	Infection period	Recovery period	Case 1	Case 2	Clean days
TVOCs	36.1 ± 21.0	31.9 ± 18.1	39.8 ± 22.4	48.4 ± 20.4	67.6 ± 19.6	17.5 ± 9.5
Alkanes	16.8 ± 9.2	15.0 ± 8.4	18.4 ± 9.5	23.1 ± 10.0	29.5 ± 8.4	9.2 ± 5.6
Alkenes	4.1 ± 2.7	3.8 ± 2.6	4.4 ± 2.7	6.5 ± 2.9	7.0 ± 2.6	1.7 ± 1.3
Alkynes	3.1 ± 2.0	2.7 ± 1.7	3.4 ± 2.1	4.3 ± 2.0	5.8 ± 1.9	1.3 ± 0.8
Aromatics	2.1 ± 2.0	1.8 ± 1.5	2.3 ± 2.2	3.0 ± 1.8	4.9 ± 2.8	0.7 ± 0.5
Halogenated hydrocarbon	5.4 ± 3.3	4.4 ± 2.3	6.2 ± 3.8	6.0 ± 1.9	10.7 ± 3.6	2.7 ± 1.4
OVOCs	4.6 ± 3.2	3.5 ± 2.7	5.1 ± 3.5	5.0 ± 2.4	9.7 ± 2.8	1.9 ± 1.1

with daily average $PM_{2.5} = 181.5\,\mu g\,m^{-3}$) were selected as they represent the pollution events in the infection and recovery periods, respectively, due to their long duration and high-pollution levels. Any day with a $PM_{2.5}$ concentration lower than $35\,\mu g\,m^{-3}$ (China's Class I standard) is considered a clean day.

As for the two representative pollution processes (case 1 during the infection period and case 2 during the recovery period), the concentration of TVOCs in case 1 and case 2 was 48.4 ± 20.4 and 67.6 ± 19.6 ppbv (Fig. 2), respectively, and increased by 63 % and 188 % compared with values during clean days. The average concentrations of $PM_{2.5}$ and TVOCs during case 2 were 1.3 and 1.8 times the values in case 1. The highest-volume contributions of alkanes were found both in case 1 (48 %) and case 2 (44 %), consistent with the results in the Yangtze River Delta region (36 %–43 %; Liu et al., 2023). While alkenes exhibited higher-volume percentages of 13 % in case 1, followed by halogenated hydrocarbon (12 %) and OVOCs (10 %). Higher-volume percentages of alkanes and alkenes in case 1 were similar to the results in the gasoline evaporation site in winter (Niu et al., 2022). Equivalent volume contribution of halogenated hydrocarbon and OVOCs (15 %) were found in case 2, followed by alkenes (10 %). Although aromatic hydrocarbons have the lowest-volumetric contribution (6 % in case 1 and 7 % in case 2), they show the largest increase from clean days to pollution.

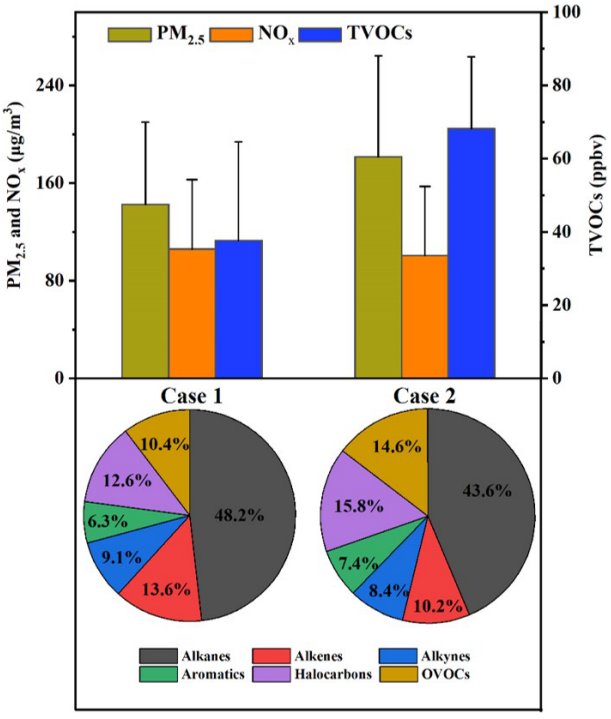

Figure 2. The concentration of $PM_{2.5}$, NO_x, TVOCs, and the composition ratio of VOCs in case 1 and case 2.

3.2 Source analysis of VOCs

Specific VOC ratios can be used for the initial source identification of VOCs and the determination of photochemical ages of air masses (Monod et al., 2001; An et al., 2014; Li et al., 2019). In this study, the ratios of toluene / benzene (T / B), isopentane / *n*-pentane, isobutane / *n*-butane, and *m*/*p*-xylene / ethylbenzene (X / E) were selected to initially identify the potential sources of VOCs (Fig. 3). Concentrations of selected pollutants and ratios used are shown in Table S1.

The toluene-to-benzene ratio (T / B ratio) was widely used to assess the relative importance of different sources. Specifically, T / B ratio with a value of 1.3–3.0 was observed in vehicle emissions for vehicles with different fuel types (Schauer et al., 2002; Wang et al., 2015). The reported T / B ratio for combustion processes was between 0.13 and 0.7 (Li et al., 2011; Wang et al., 2014). The mean value of the T / B ratio for the entire period was 1.0, with the majority of the data (99 %) falling between 0.1 and 3.0 and concentrated within the 0.7–1.3 range (49 %). This suggests that both traffic emissions and combustion may be significant sources of VOCs. It should be noted that this analytical approach is not without limitations. The ratios observed here do not exclude linear combinations from other sources. Consequently, an in-depth examination of the sources of VOCs was conducted using the PMF model in the next section.

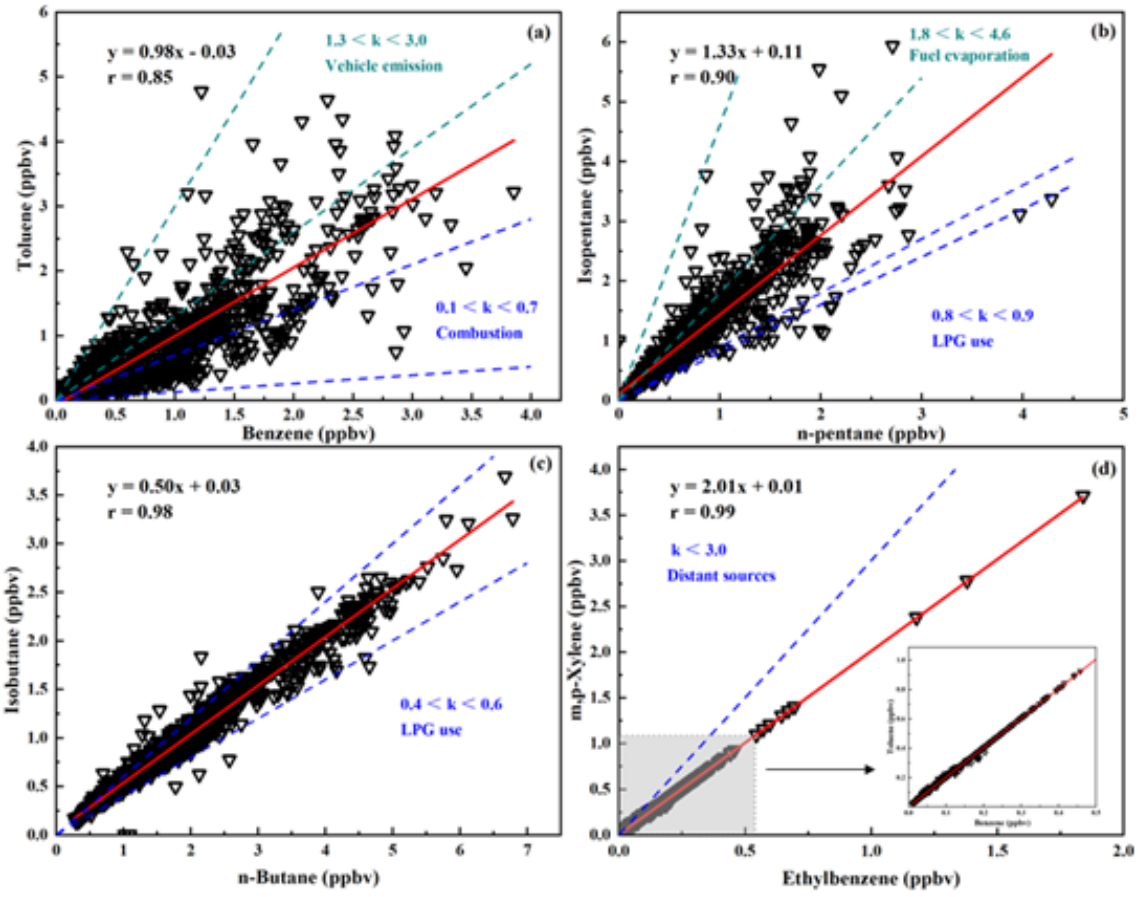

Figure 3. Correlation analysis between specific VOC species.

The isopentane / *n*-pentane concentration ratios of 0.6–0.8 represent mainly coal combustion emissions, ratios of 0.8–0.9 represent LPG emissions, 2.2–3.8 represent vehicle exhaust emissions, and 1.8–4.6 represent fuel evaporation (Conner et al., 1995; Liu et al., 2008; Li et al., 2019). The sources of isopentane and *n*-pentane in this study were intricate and multifaceted. The mean isopentane / *n*-pentane ratio was 1.4, with the majority of data points (99 %) falling within the range of 0.1–4.6, with a notable concentration in the 0.8 to 1.8 interval. This indicates that pentane is susceptible to a combination of LPG emissions and fuel evaporation. However, the proportion of pentane may also be affected by a combination of coal combustion emissions and vehicle exhaust.

Isobutane / *n*-butane concentration ratios of 0.2–0.3 represent vehicle emissions, 0.4–0.6 represent LPG usage, and 0.6–1.0 represent natural gas emissions (Russo et al., 2010; Zheng et al., 2018). The mean isobutane / *n*-butane ratio in this study was 0.5, with the majority of data points (99 %) falling within the 0.4–0.6 range, indicating that VOCs at the observation sites were significantly influenced by the use of LPG (Shao et al., 2016; Zeng et al., 2023). This result can also be caused by a combination of vehicle exhaust and natural gas emissions.

The ratio of X / E can be used to infer the photochemical age of the air mass. X / E ratios around 2.5–2.9 are typical of urban areas, indicating that VOCs are mainly from the urban area (fresh air mass) (Kumar et al., 2018). When this ratio is significantly lower than 3.0, it indicates that VOCs are mainly transported from distant sources (aging air masses) (Kumar et al., 2018). The average X / E value in this study was 2.0 (Fig. 3d), indicating low-photochemical activity and aging of the air mass at the observation site. Potential source analyses also indicate that air masses are affected by long-range transport (Fig. S4).

Figure 4 shows the chemical profiles of individual VOCs resolved by the PMF model during the entire observation period. These five factors, eventually selected as potential sources for the observed VOCs, are (1) fuel evaporation, (2) solvent usage, (3) vehicular emission, (4) industrial source, and (5) combustion. These five factors have been commonly reported before, e.g., in Shijiazhuang, northern China (Guan et al., 2023) and in Beijing (Cui et al., 2022).

Alkanes of C_4–C_6 substances were predominant in factor (1), including 2-methylpentane, 3-methylpentane, isobutane,

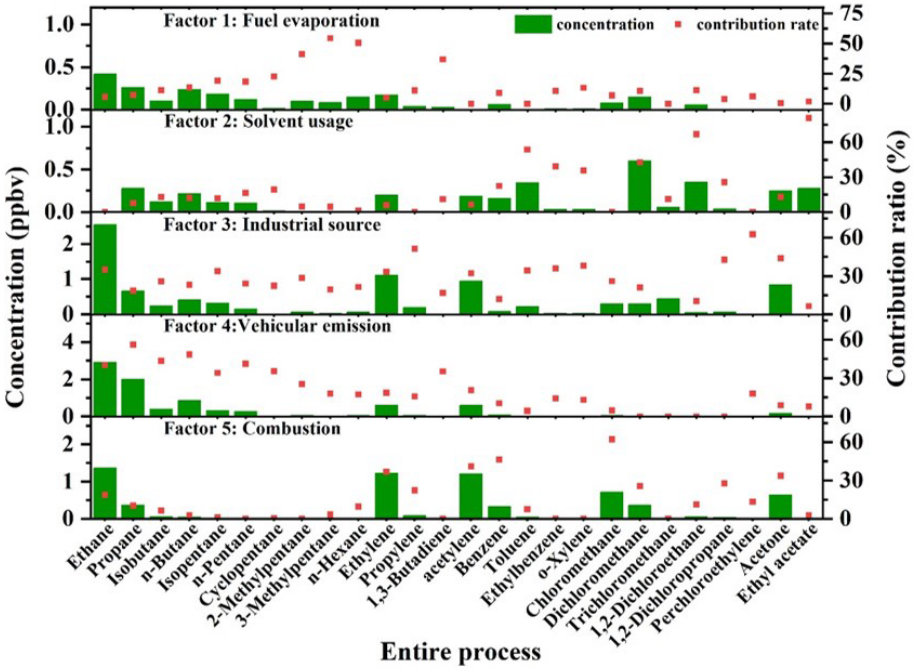

Figure 4. Concentration of VOC species in each factor and contribution to each source.

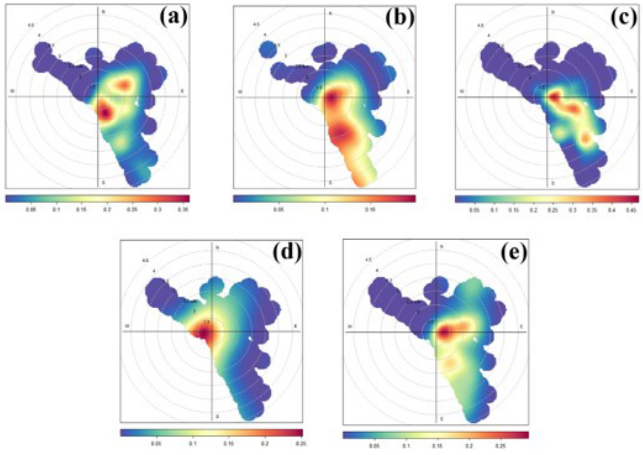

Figure 5. CPF plots of five VOC sources obtained using the PMF model. **(a)** Fuel evaporation. **(b)** Solvent usage. **(c)** Industrial source. **(d)** Vehicular emission. **(e)** Combustion.

n-butane, isopentane, and *n*-pentane from oil and gas (Xiong et al., 2020). Figure S5 shows that emissions from this source peak at midday, when fuel volatilization is high. The conditional probability function (CPF) plot shows that southeast is the dominant direction at wind speeds $< 2\,\mathrm{m\,s^{-1}}$ (Fig. 5a). Therefore, factor (1) was identified as the source of oil and gas volatilization.

The contribution of benzene, toluene, methylene chloride, 1,2-dichloroethane, and ethyl acetate was high in factor (2). It has been shown that benzene, toluene, ethylbenzene, and xylene are important components in the use of solvents (Li et al., 2015); methylene chloride is often used as a chemical solvent, while esters are mostly used as industrial solvents or adhesives (Li et al., 2015). Factor (2) is determined to be a solvent usage source. The CPF plot shows that due east is the main emission direction at wind speeds $< 2\,\mathrm{m\,s^{-1}}$, and southeast is the main source at wind speeds $> 22\,\mathrm{m\,s^{-1}}$ (Fig. 5b).

Factor (3) contains predominantly C_3–C_8 alkanes, olefins, and alkynes and relatively high concentrations of benzene. These substances are usually emitted by industrial processes (Shao et al., 2016), so factor (4) is defined as an industrial source. The CPF plots indicate that a local source at low wind speeds is the dominant sources (Fig. 5c).

Factor (4) is characterized by relatively high levels of C_2–C_6 low-carbon alkanes (ethane, propane, isopentane, *n*-pentane, isobutane, and *n*-butane), olefins (ethylene and propylene), and benzene and toluene, which are important automotive exhaust tracers (Song et al., 2021; D. Zhang et al., 2021). Ethylene and propylene are important components derived from vehicle-related activities. Previous studies of VOCs in Zhengzhou have shown a high percentage of VOCs emitted from gasoline vehicles, with the main source of alkanes being on-road mobile sources (Bai et al., 2020). The daily variation in this source in Fig. S5 shows a bimodal trend, with peaks occurring in the morning and evening peaks of traffic, consistent with motor vehicle emissions. Figure 5d shows that this source is mainly from the west, where wind speeds are below $2\,\mathrm{m\,s^{-1}}$, and in this direction, there are a number

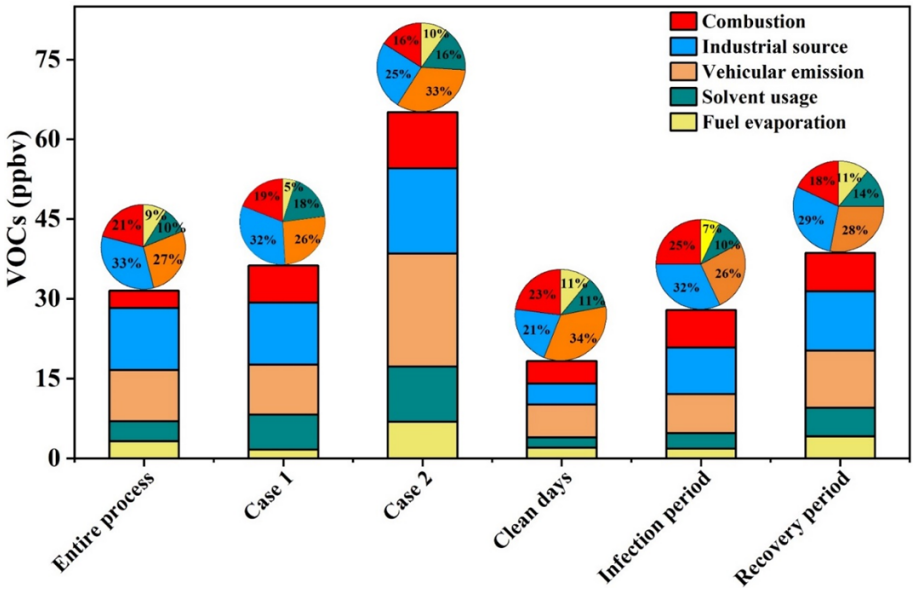

Figure 6. Contribution of each source to VOCs for different processes.

of urban arterial roads with high-traffic volumes. Therefore, factor (4) was defined as vehicular emission source.

The highest contribution to factor (5) is chloromethane (62 %). Benzene (46 %) and acetylene (41 %) also contribute highly to factor (5). Chloromethane is the key tracer for biomass combustion, and acetylene is the key tracer for coal combustion (Xiong et al., 2020). Therefore, factor (5) is defined as a combustion source. The CPF plot shows that at wind speeds $< 2\,\mathrm{m\,s^{-1}}$, the northeasterly direction is the dominant source direction (Fig. 5e).

Figure S6 compares the differences in PMF source profiles between the Omicron infection period and the recovery period, as well as between the pollution day and the clean day. We present the concentrations of the five main VOCs in all five factors in Table S2. Ethane (vehicular emission), 2-methylpentane (fuel evaporation), benzene (industry source), chloromethane (combustion), and ethyl acetate (solvent usage) were selected as tracers for the five sources. Ethane concentration in case 2 (5.9 ppbv) is much higher than in other processes, and ethane concentration during the recovery period (3.4 ppbv) is also higher than during the infection period (2.4 ppbv), which may to some extent reflect increased vehicular emissions during the recovery period.

Concentrations of most species were significantly higher during the recovery period than during the infection period. The representative pollution processes in both periods showed the same results as well, with 79 % higher concentration of TVOCs in case 2 (65.1 ppbv) compared to case 1 (36.3 ppbv) (Fig. 6). While industry was the dominant source of VOCs in case 1, by case 2 the motorized sources reached a concentration value of 21.2 ppbv, accounting for 33 % of the observed VOCs, and became the dominant source of emissions. This is consistent with the fact that people's mobility activities increased after the epidemic entered the recovery period. As a group of VOC species with the highest-concentration share, ethane and propane contributed more to the motor vehicle source on clean days than other processes, which also resulted in 34 % motor vehicle source share for clean days.

3.3 SOAP

VOCs are estimated to contribute about 16 %–30 % or more of $PM_{2.5}$ by mass through SOA production (Huang et al., 2014). Therefore, by calculating the SOAP value, the influence of different sources on $PM_{2.5}$ production can be reflected to a certain extent.

We have included quantitative analysis for SOAP as well. Figure 7 shows the SOAP concentrations and contribution rates of the top 10 species throughout the entire process, during two pollution processes, and clean days. The top 10 species all reached close to 100 % of the total SOAP contribution, with case 1 reaching 98 %. In each process, the composition of the top 10 substances is essentially the same. Aromatic hydrocarbons contributed the most, with benzene, toluene, ethylbenzene, and xylenes (BTEX) always occupying the top five positions and toluene the most. The SOAP values of the top 10 contributing species for the two polluting processes are shown in Tables S3 and S4. Toluene, the highest-contributing species, reached a SOAP value of $49.4\,\mu g\,m^{-3}$ in the most polluted case 2, which was 3.2 times higher than the SOAP sum of all species on the clean day ($15.5\,\mu g\,m^{-3}$). The SOAP value for case 1, which is also a contaminated process, was $67\,\mu g\,m^{-3}$, and the main species (m/p-xylene: $9.8\,\mu g\,m^{-3}$; benzene: $8.5\,\mu g\,m^{-3}$), including

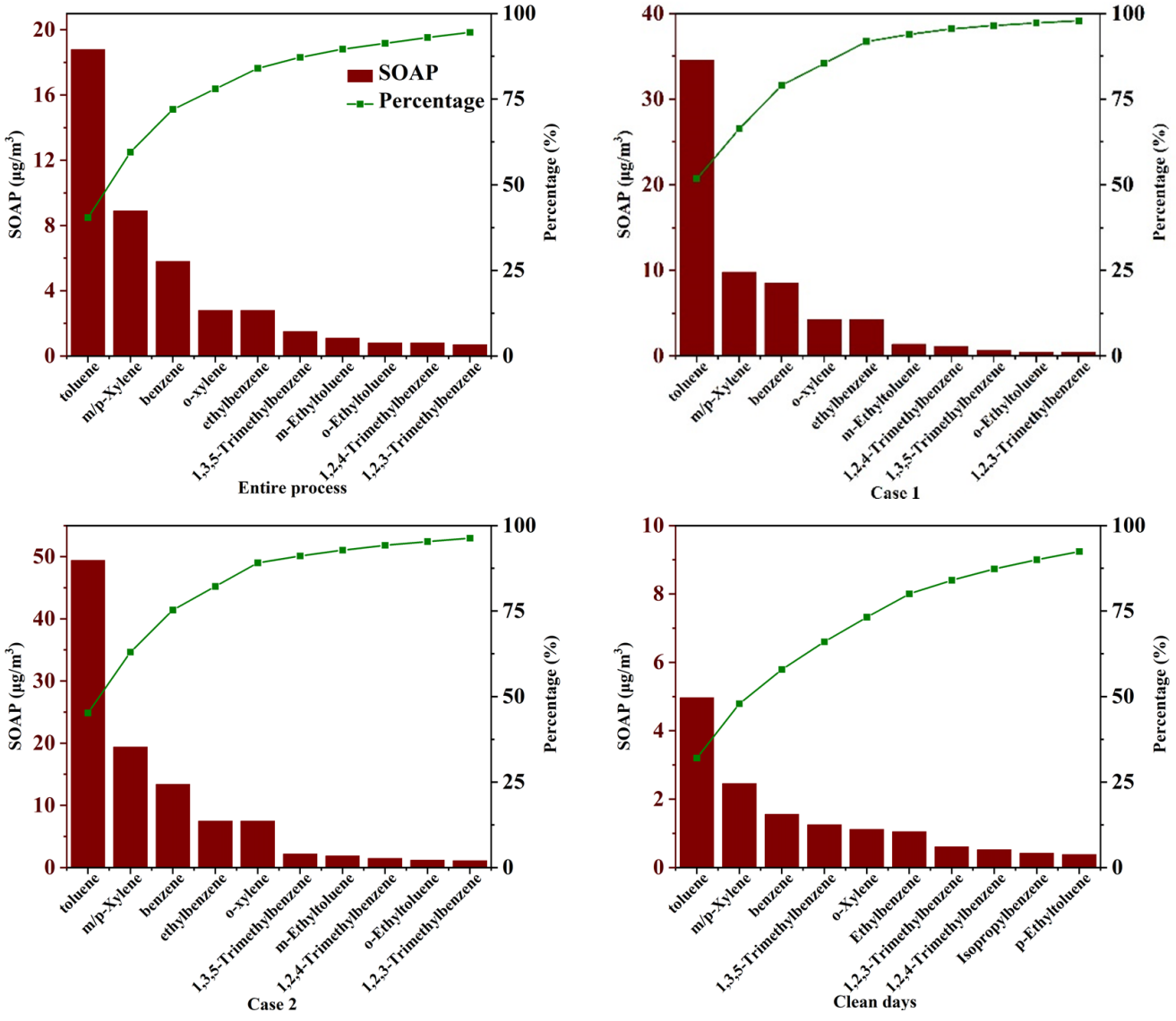

Figure 7. Dominant SOAP species for different processes.

toluene (34.6 μg m^{-3}), were lower than those for case 2 (*m*/*p*-xylene: 19.4 μg m^{-3}; benzene: 13.4 μg m^{-3}).

Figure 8 shows the SOAP calculated after the source resolution of the two pollution processes by PMF for clean days, respectively. In case 1, the industrial source is the dominant source, with a contribution ratio of 63 %. In case 2, the pollution sources exhibit a more evenly distributed contribution, where the solvent usage and fuel evaporation sources emerge as the primary contributors to SOAP, with their respective contribution levels rising to 32 % and 26 %. Case 1 was during the infection period, when social activities had not yet returned to normal. In case 2, when society had basically returned to normal, the increase in emissions from various sources resulted in a more balanced distribution of SOAP contributions and caused more severe $PM_{2.5}$ pollution. In addition, a few days before case 2, the Zhengzhou Municipal People's Government initiated the Heavy Pollution Weather Level II response (https://sthjj.zhengzhou.gov.cn/tzgg/7037130.jhtml, last access: 14 July 2024) and introduced control measures for emissions from industrial and mobile sources, which resulted in a significant reduction in SOAP levels from industrial and motorized sources in case 2. The clean day result, with a SOAP of 8.8 μg m^{-3}, also indicates that industrial and solvent usage sources are the most dominant SOAP sources. The primary sources of aromatic compounds, which are the most significant contributors to SOAP, are solvent usage and industrial process emissions. This finding aligns with the results of other studies (Wu et al., 2017). Consequently, it is imperative to implement mea-

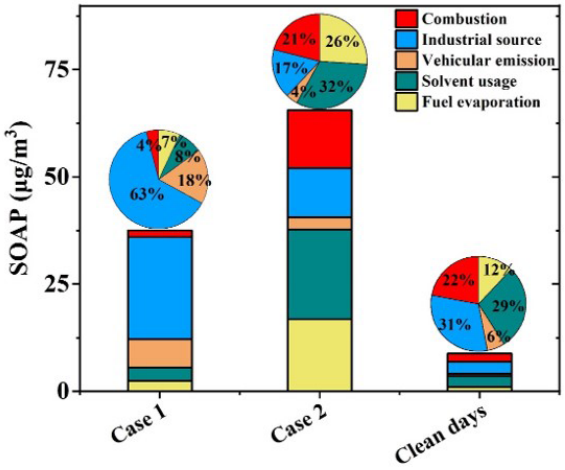

Figure 8. SOAP value and the contribution ratio of each process.

sures to reduce $PM_{2.5}$ pollution by regulating emissions from industrial and solvent usage sources.

4 Conclusions

Continuous observation of VOCs during the Omicron epidemic was carried out at an urban site in polluted Zhengzhou from 1 December 2022 to 31 January 2023. The daily average concentration of $PM_{2.5}$ ranged from 53.5 to 239.4 $\mu g\,m^{-3}$, with an average value of $111.5 \pm 45.1\,\mu g\,m^{-3}$ during the whole period. The concentration of TVOCs ranged from 15.6 to 57.1 ppbv (parts per billion by volume), with an average of 36.1 ± 21.0 ppbv, which is higher than the same period in the previous year (27.9 ± 12.7 ppbv; Lai et al., 2024). Two representative contamination processes were identified (case 1 during the infection period and case 2 during the recovery period). While the meteorological conditions of the two pollution processes are relatively similar, the specific impacts caused thereby have yet to be determined. The concentration of TVOCs in case 1 and case 2 were 48.4 ± 20.4 and 67.6 ± 19.6 ppbv, respectively, and increased by 63 % and 188 % when compared with the values during clean days. The average concentrations of $PM_{2.5}$ and TVOCs during case 2 were 1.3 and 1.8 times of the values in case 1. This is consistent with the observed increase in pollutant emissions following people's return to a normal and social life after the period of Omicron infections. The highest-volume contributions of alkanes were found both in case 1 (48 %) and case 2 (44 %). Though the volume contribution of aromatics was the lowest (6 % in case 1 and 7 % in case 2), the highest-increase ratio was found from clean days to polluted episodes. Low WS and high RH were the main meteorological reasons for the occurrence of pollution. Analyzing the sources of VOCs revealed that VOCs were found to be affected by a combination of local emissions and regional transport. The primary sources of atmospheric VOCs in Zhengzhou were identified as industrial emissions (32 %), vehicle emissions (27 %), and combustion (21 %). Significant discrepancies were observed in the sources of VOCs between the two pollution processes. In case 1, industrial emissions constituted the primary source of VOCs, accounting for 32 % of the total VOC concentration. In contrast, in case 2, the proportion of vehicle emissions increased to 33 %, representing the primary source of VOCs.

A further analysis of the effect of VOCs on SOA generation reveals that aromatic compounds are the primary contributors to SOAP, with BTEX being the predominant contributor throughout the period. The SOAP values reached 37.6 and $65.6\,\mu g\,m^{-3}$ in case 1 and case 2, respectively. In case 1, the greatest contribution to SOAP was made by industrial sources (63 %, $23.8\,\mu g\,m^{-3}$), while vehicular sources, which constituted the second most important source, accounted for only 18 %. In case 2, the contribution of each VOC source was more evenly distributed, with solvent use sources and fuel evaporation sources representing the primary contributors to SOAP and accounting for 32 % ($20.9\,\mu g\,m^{-3}$) and 26 % ($16.8\,\mu g\,m^{-3}$), respectively. The SOAP result for the clean day was $8.8\,\mu g\,m^{-3}$, with industrial sources and solvent use still being the primary contributors. Therefore, the industrial and solvent use sectors are the predominant sources of pollutants during this observation. The aforementioned results substantiate the considerable impact of elevated emissions from all sources on the exacerbation of pollution following the conclusion of the Omicron infection.

Data availability. The data set is available to the public and can be accessed upon request from Ruiqin Zhang (rqzhang@zzu.edu.cn).

Supplement. The supplement related to this article is available online at: https://doi.org/10.5194/acp-24-13587-2024-supplement.

Author contributions. BZ: data curation, methodology, formal analysis, and writing (original draft). DZ and ZD: data curation, formal analysis, and review and editing. XS: data curation and formal analysis. RZ: supervision, writing (review and editing), and funding acquisition. XL: formal analysis, investigation, supervision, and writing (review and editing).

Competing interests. The contact author has declared that none of the authors has any competing interests.

Disclaimer. Publisher's note: Copernicus Publications remains neutral with regard to jurisdictional claims made in the text, published maps, institutional affiliations, or any other geographical representation in this paper. While Copernicus Publications makes ev-

ery effort to include appropriate place names, the final responsibility lies with the authors.

Financial support. This research has been supported by the Natural Science Foundation of Henan Province (grant no. 232300421395) and the National Key Research and Development Program of China (grant no. 2017YFC0212400).

Review statement. This paper was edited by Kelvin Bates and reviewed by three anonymous referees.

References

An, J., Zhu, B., Wang, H., Li, Y., Lin, X., and Yang, H.: Characteristics and source apportionment of VOCs measured in an industrial area of Nanjing, Yangtze River Delta, China, Atmos. Environ., 97, 206–214, https://doi.org/10.1016/j.atmosenv.2014.08.021, 2014.

Bai, L., Lu, X., Yin, S., Zhang, H., Ma, S., Wang, C., Li, Y., and Zhang, R.: A recent emission inventory of multiple air pollutant, $PM_{2.5}$ chemical species and its spatial-temporal characteristics in central China, J. Clean. Prod., 269, 122114, https://doi.org/10.1016/j.jclepro.2020.122114, 2020.

Buzcu, B. and Fraser, M. P.: Source identification and apportionment of volatile organic compounds in Houston, TX, Atmos. Environ., 40, 2385–2400, https://doi.org/10.1016/j.atmosenv.2005.12.020, 2006.

CCDCP: National epidemic of novel coronavirus infections, Chinese Center for Disease Control and Prevention, https://www.chinacdc.cn/jkyj/crb2/yl/xxgzbdgr/xggrqk/202409/t20240906_297054.html, last access: 18 November 2023.

Conner, T. L., Lonneman, W. A., and Seila, R. L.: Transportation-related volatile hydrocarbon source profiles measured in atlanta, J. Air Waste Manage. Assoc., 45, 383–394, https://doi.org/10.1080/10473289.1995.10467370, 1995.

Cui, L., Wu, D., Wang, S., Xu, Q., Hu, R., and Hao, J.: Measurement report: Ambient volatile organic compound (VOC) pollution in urban Beijing: characteristics, sources, and implications for pollution control, Atmos. Chem. Phys., 22, 11931–11944, https://doi.org/10.5194/acp-22-11931-2022, 2022.

Derwent, R. G., Jenkin, M. E., Utembe, S. R., Shallcross, D. E., Murrells, T. P., and Passant, N. R.: Secondary organic aerosol formation from a large number of reactive man-made organic compounds, Sci. Total Environ., 408, 3374–3381, https://doi.org/10.1016/j.scitotenv.2010.04.013, 2010.

Duan, S., Jiang, N., Yang, L., and Zhang, R.: Transport Pathways and Potential Sources of $PM_{2.5}$ During the Winter in Zhengzhou, Environm. Sci., 40, 86–93, https://doi.org/10.13227/j.hjkx.201805187, 2019.

Gao, J., Zhang, J., Li, H., Li, L., Xu, L., Zhang, Y., Wang, Z., Wang, X., Zhang, W., Chen, Y., Cheng, X., Zhang, H., Peng, L., Chai, F., and Wei, Y.: Comparative study of volatile organic compounds in ambient air using observed mixing ratios and initial mixing ratios taking chemical loss into account – A case study in a typical urban area in Beijing, Sci. Total Environ., 628–629, 791–804, https://doi.org/10.1016/j.scitotenv.2018.01.175, 2018.

Guan, Y., Liu, X., Zheng, Z., Dai, Y., Du, G., Han, J., Hou, L. A., and Duan, E.: Summer O_3 pollution cycle characteristics and VOCs sources in a central city of Beijing-Tianjin-Hebei area, China, Environ. Pollut., 323, 121293, https://doi.org/10.1016/j.envpol.2023.121293, 2023.

Huang, R., Zhang, Y., Bozzetti, C., Ho, K., Cao, J., Han, Y., Daellenbach, K., Slowik, J., Platt, S., Canonaco, F., Zotter, P., Wolf, R., Pieber S., Bruns, E., Crippa, M., Ciarelli, G., Piazzalunga, A., Schwikowski, M., Abbaszade, G., Schnellekreis, J., Zimmermann, R., An, Z., Szidat, S., and Baltensperger, U.: High secondary aerosol contribution to particulate pollution during haze events in China, Nature, 514, 218–22, https://doi.org/10.1038/nature13774, 2014.

Hui, L., Liu, X., Tan, Q., Feng, M., An, J., Qu, Y., Zhang, Y., Deng, Y., Zhai, R., and Wang, Z.: VOC characteristics, chemical reactivity and sources in urban Wuhan, central China, Atmos. Environ., 224, 117340, https://doi.org/10.1016/j.atmosenv.2020.117340, 2020.

Jensen, A., Liu, Z., Tan, W., Dix, B., Chen, T., Koss, A., Zhu, L., Li, L., and de Gouw, J.: Measurements of volatile organic compounds during the COVID-19 lockdown in Changzhou, China, Geophys. Res. Lett., 48, e2021GL095560, https://doi.org/10.1029/2021GL095560, 2021.

Jiang, N., Hao, X., Hao, Q., Wei, Y., Zhang, Y., Lyu, Z., and Zhang, R.: Changes in secondary inorganic ions in $PM_{2.5}$ at different pollution stages before and after COVID-19 control, Environm. Sci., 44, 2430–2440, https://doi.org/10.13227/j.hjkx.202206170, 2023.

Kumar, A., Singh, D., Kumar, K., Singh, B. B., and Jain, V. K.: Distribution of VOCs in urban and rural atmospheres of subtropical India: Temporal variation, source attribution, ratios, OFP and risk assessment, Sci. Total Environ., 613–614, 492–501, https://doi.org/10.1016/j.scitotenv.2017.09.096, 2018.

Lai, M., Zhang, D., Yin, S., Song, X., and Zhang, R.: Pollution characteristics, source apportionment and activity analysis of atmospheric VOCs during winter and summer pollution in Zhengzhou City, Environm. Sci., 4108, 3500–3510, https://doi.org/10.13227/j.hjkx.202001133, 2024.

Li, B., Ho, S. S. H., Gong, S., Ni, J., Li, H., Han, L., Yang, Y., Qi, Y., and Zhao, D.: Characterization of VOCs and their related atmospheric processes in a central Chinese city during severe ozone pollution periods, Atmos. Chem. Phys., 19, 617–638, https://doi.org/10.5194/acp-19-617-2019, 2019.

Li, J., Lu, K., Lv, W., Li, J., Zhong, L., Ou, Y., Chen, D., Huang, X., and Zhang, Y.: Fast increasing of surface ozone concentrations in Pearl River Delta characterized by a regional air quality monitoring network during 2006–2011, J. Environ. Sci., 26, 23–36, https://doi.org/10.1016/S1001-0742(13)60377-0, 2014.

Li, J., Xie, S. D., Zeng, L. M., Li, L. Y., Li, Y. Q., and Wu, R. R.: Characterization of ambient volatile organic compounds and their sources in Beijing, before, during, and after Asia-Pacific Economic Cooperation China 2014, Atmos. Chem. Phys., 15, 7945–7959, https://doi.org/10.5194/acp-15-7945-2015, 2015.

Li, J., Deng, S., Tohti, A., Li, G., Yi, X., Lu, Z., Liu, J., and Zhang, S.: Spatial characteristics of VOCs and their ozone and secondary organic aerosol formation potentials in autumn and winter in the Guanzhong Plain, China, Environ. Res., 211, 113036, https://doi.org/10.1016/j.envres.2022.113036, 2022.

Li, X., Wang, S., and Hao, J.: Characteristics of volatile organic compounds (VOCs) emitted from biofuel combustion in China, Environm. Sci., 32, 3515–3521, 2011.

Li, Y., Yin, S., Zhang R., Yu, S., Yang, J., and Zhang, D.: Characteristics and source apportionment of atmospheric VOCs at different pollution levels in winter in an urban area in Zhengzhou, Environm. Sci., 4108, 3500–3510, https://doi.org/10.13227/j.hjkx.202001133, 2020.

Liu, Y., Shao, M., Fu, L., Lu, S., Zeng, L., and Tang, D.: Source profiles of volatile organic compounds (VOCs) measured in China: Part I, Atmos. Environ., 42, 6247–6260, https://doi.org/10.1016/j.atmosenv.2008.01.070, 2008.

Liu, Y., Li, X., Tang, G., Wang, L., Lv, B., Guo, X., and Wang, Y.: Secondary organic aerosols in Jinan, an urban site in North China: Significant anthropogenic contributions to heavy pollution, J. Environ. Sci., 80, 107–115, https://doi.org/10.1016/j.jes.2018.11.009, 2019.

Liu, Y., Song, M., Liu, X., Zhang, Y., Hui, L., Kong, L., Zhang, Y., Zhang, C., Qu, Y., An, J., Ma, D., Tan, Q., and Feng, M.: Characterization and sources of volatile organic compounds (VOCs) and their related changes during ozone pollution days in 2016 in Beijing, China, Environ. Pollut., 257, 113599, https://doi.org/10.1016/j.envpol.2019.113599, 2020.

Liu, Z., Hu, K., Zhang, K., Zhu, S., Wang, M., and Li, L.: VOCs sources and roles in O_3 formation in the central Yangtze River Delta region of China, Atmos. Environ., 302, 119755, https://doi.org/10.1016/j.atmosenv.2023.119755, 2023.

Ma, Q., Wang, W., Wu, Y., Wang, F., Jin, L., Song, Y., Han, Y., Zhang, R., and Zhang, D.: Haze caused by NO_x oxidation under restricted residential and industrial activities in a mega city in the south of North China Plain, Chemosphere, 305, 135489, https://doi.org/10.1016/j.chemosphere.2022.135489, 2022.

Merino, M., Marinescu, M., Cascajo, A., Carretero, J., and Singh, D.: Evaluating the spread of Omicron COVID-19 variant in Spain, Future Gener. Comp. Sy., 149, 547–561, https://doi.org/10.1016/j.future.2023.07.025, 2023.

Monod, A., Sive, B. C., Avino, P., Chen, T., Blake, D. R., and Sherwood Rowland, F.: Monoaromatic compounds in ambient air of various cities: a focus on correlations between the xylenes and ethylbenzene, Atmos. Environ., 35, 135–149, https://doi.org/10.1016/S1352-2310(00)00274-0, 2001.

Mozaffar, A., Zhang, Y.-L., Fan, M., Cao, F., and Lin, Y.-C.: Characteristics of summertime ambient VOCs and their contributions to O_3 and SOA formation in a suburban area of Nanjing, China, Atmos. Res., 240, 104923, https://doi.org/10.1016/j.atmosres.2020.104923, 2020.

Mu, L., Feng, C., Li, Y., Li, X., Liu, T., Jiang, X., Liu, Z., Bai, H., and Liu, X.: Emission factors and source profiles of VOCs emitted from coke production in Shanxi, China, Environ. Pollut., 335, 122373, https://doi.org/10.1016/j.envpol.2023.122373, 2023.

Niu, Y., Yan, Y., Chai, J., Zhang, X., Xu, Y., Duan, X., Wu, J., and Peng, L.: Effects of regional transport from different potential pollution areas on volatile organic compounds (VOCs) in Northern Beijing during non-heating and heating periods, Sci. Total Environ., 836, 155465, https://doi.org/10.1016/j.scitotenv.2022.155465, 2022.

Norris, G., Duvall, R., Brown, S., and Bai, S.: EPA Positive Matrix Factorization (PMF) 5.0 Fundamentals and User Guide. U.S. Environmental Protection Agency, Washington, DC, EPA/600/R-14/108 (NTIS PB2015-105147), 2014.

Paatero, P., Eberly, S., Brown, S. G., and Norris, G. A.: Methods for estimating uncertainty in factor analytic solutions, Atmos. Meas. Tech., 7, 781–797, https://doi.org/10.5194/amt-7-781-2014, 2014.

Pei, C., Yang, W., Zhang, Y., Song, W., Xiao, S., Wang, J., Zhang, J., Zhang, T., Chen, D., Wang, Y., Chen, Y., and Wang, X.: Decrease in ambient volatile organic compounds during the COVID-19 lockdown period in the Pearl River Delta region, south China, Sci. Total Environ., 823, 153720, https://doi.org/10.1016/j.scitotenv.2022.153720, 2022.

Petersen, M. S., Í Kongsstovu, S., Eliasen, E. H., Larsen, S., Hansen, J. L., Vest, N., Dahl, M. M., Christiansen, D. H., Møller, L. F., and Kristiansen, M. F.: Clinical characteristics of the Omicron variant – results from a Nationwide Symptoms Survey in the Faroe Islands, Int. J. Infect. Dis., 122, 636–643, https://doi.org/10.1016/j.ijid.2022.07.005, 2022.

Qi, J., Mo, Z., Yuan, B., Huang, S., Huangfu, Y., Wang, Z., Li, X., Yang, S., Wang, W., Zhao, Y., Wang, X., Wang, W., Liu, K., and Shao, M.: An observation approach in evaluation of ozone production to precursor changes during the COVID-19 lockdown, Atmos. Environ., 262, 118618, https://doi.org/10.1016/j.atmosenv.2021.118618, 2021.

Russo, R. S., Zhou, Y., White, M. L., Mao, H., Talbot, R., and Sive, B. C.: Multi-year (2004–2008) record of nonmethane hydrocarbons and halocarbons in New England: seasonal variations and regional sources, Atmos. Chem. Phys., 10, 4909–4929, https://doi.org/10.5194/acp-10-4909-2010, 2010.

Sahu, L. K., Tripathi, N., Gupta, M., Singh, V., Yadav, R., and Patel, K.: Impact of COVID-19 Pandemic lockdown in ambient concentrations of aromatic volatile organic compounds in a metropolitan city of western India, J. Geophys. Res.-Atmos., 127, e2022JD036628, https://doi.org/10.1029/2022JD036628, 2022.

Schauer, J., Kleeman, M., Cass, G., and Simoneit, B.: Measurement of emissions from air pollution sources. 5. C_1–C_{32} organic compounds from gasoline-powered motor vehicles, Environ. Sci. Technol., 36, 1169–1180, https://doi.org/10.1021/es0108077, 2002.

Shao, P., An, J., Xin, J., Wu, F., Wang, J., Ji, D., and Wang, Y.: Source apportionment of VOCs and the contribution to photochemical ozone formation during summer in the typical industrial area in the Yangtze River Delta, China, Atmos. Res., 176–177, 64–74, https://doi.org/10.1016/j.atmosres.2016.02.015, 2016.

Shi, Y., Liu, C., Zhang, B., Simayi, M., Xi, Z., Ren, J., and Xie, S.: Accurate identification of key VOCs sources contributing to O_3 formation along the Liaodong Bay based on emission inventories and ambient observations, Sci. Total Environ., 844, 156998, 10.1016/j.scitotenv.2022.156998, 2022.

Singh, B., Sohrab, S., Athar, M., Alandijany, T., Kumari, S., Nair, A., Kumari, S., Mehra, K., Chowdhary, K., Rahman, S., and Azhar, E.: Substantial changes in selected volatile organic compounds (VOCs) and associations with health risk assessments in industrial areas during the COVID-19 Pandemic, Toxics, 11, 165, https://doi.org/10.3390/toxics11020165, 2023a.

Singh, B., Singh, M., Ulman, Y., Sharma, U., Pradhan, R., Sahoo, J., Padhi, S., Chandra, P., Koul, M., Tripathi, P., Ku-

mar, D., and Masih, J.: Distribution and temporal variation of total volatile organic compounds concentrations associated with health risk in Punjab, India, Case Studies in Chemical and Environmental Engineering, 8, 100417, https://doi.org/10.1016/j.cscee.2023.100417, 2023b.

Song, M., Li, X., Yang, S., Yu, X., Zhou, S., Yang, Y., Chen, S., Dong, H., Liao, K., Chen, Q., Lu, K., Zhang, N., Cao, J., Zeng, L., and Zhang, Y.: Spatiotemporal variation, sources, and secondary transformation potential of volatile organic compounds in Xi'an, China, Atmos. Chem. Phys., 21, 4939–4958, https://doi.org/10.5194/acp-21-4939-2021, 2021.

Song, X., Zhang, D., Li, X., Lu, X., Wang, M., Zhang, B., and Zhang, R.: Simultaneous observations of peroxyacetyl nitrate and ozone in Central China during static management of COVID-19: Regional transport and thermal decomposition, Atmos. Res., 294, 106958, https://doi.org/10.1016/j.atmosres.2023.106958, 2023.

Song, Y., Shao, M., Liu, Y., Lu, S., Kuster, W., Goldan, P., and Xie, S.: Source apportionment of ambient volatile organic compounds in Beijing, Environ. Sci. Technol., 41, 4348–4353, https://doi.org/10.1021/es0625982, 2007.

Wang, H., Wang, Q., Chen, J. Chen, C., Huang, C., Qiao, L. Lou, S., and Lu, J.: Do vehicular emissions dominate the source of C6–C8 aromatics in the megacity Shanghai of eastern China?, Environm. Sci., 27, 290–297, https://doi.org/10.1016/j.jes.2014.05.033, 2015.

Wang, H., Li, J., Peng, Y., Zhang, M., Che, H., and Zhang, X.: The impacts of the meteorology features on $PM_{2.5}$ levels during a severe haze episode in central-east China, Atmos. Environ., 197, 177–189, https://doi.org/10.1016/j.atmosenv.2018.10.001, 2019.

Wang, M., Zeng, L., Lu, S., Shao, M., Liu, X., Yu, X., Chen, W., Yuan, B., Zhang, Q., Hu, M., and Zhang, Z.: Development and validation of a cryogen-free automatic gas chromatograph system (GC-MS/FID) for online measurements of volatile organic compounds, Anal. Methods, 6, 9424, https://doi.org/10.1039/C4AY01855A, 2014.

Wang, M., Lu, S., Shao, M., Zeng, L., Zheng, J., Xie, F., Lin, H., Hu, K., and Lu, X.: Impact of COVID-19 lockdown on ambient levels and sources of volatile organic compounds (VOCs) in Nanjing, China, Sci. Total Environ., 757, 143823, https://doi.org/10.1016/j.scitotenv.2020.143823, 2021.

Wang, T., Xue, L., Brimblecombe, P., Lam, Y. F., Li, L., and Zhang, L.: Ozone pollution in China: A review of concentrations, meteorological influences, chemical precursors, and effects, Sci. Total Environ., 575, 1582–1596, https://doi.org/10.1016/j.scitotenv.2016.10.081, 2017.

Wu, R., Li, J., Hao, Y., Li, Y., Zeng, L., and Xie, S.: Evolution process and sources of ambient volatile organic compounds during a severe haze event in Beijing, China, Sci. Total Environ., 560–561, 62–72, https://doi.org/10.1016/j.scitotenv.2016.04.030, 2016.

Wu, W., Zhao, B., Wang, S., and Hao, J.: Ozone and secondary organic aerosol formation potential from anthropogenic volatile organic compounds emissions in China, J. Environ. Sci., 53, 224–237, https://doi.org/10.1016/j.jes.2016.03.025, 2017.

Xiong, Y., Zhou, J., Xing, Z., and Du, K.: Optimization of a volatile organic compound control strategy in an oil industry center in Canada by evaluating ozone and secondary organic aerosol formation potential, Environ. Res., 191, 110217, https://doi.org/10.1016/j.envres.2020.110217, 2020.

Yun, L., Li, C., Zhang, M., He, L., and Guo, J.: Pollution characteristics and sources of atmospheric VOCs in the coastal background area of the Pearl River Delta, Environm. Sci., 4191–4201, https://doi.org/10.13227/j.hjkx.202101155, 2021.

Zeng, X., Han, M., Ren, G., Liu, G., Wang, X., Du, K., Zhang, X., and Lin, H.: A comprehensive investigation on source apportionment and multi-directional regional transport of volatile organic compounds and ozone in urban Zhengzhou, Chemosphere, 334, 139001, https://doi.org/10.1016/j.chemosphere.2023.139001, 2023.

Zhang, C., Liu, X., Zhang, Y., Tan, Q., Feng, M., Qu, Y., An, J., Deng, Y., Zhai, R., Wang, Z., Cheng, N., and Zha, S.: Characteristics, source apportionment and chemical conversions of VOCs based on a comprehensive summer observation experiment in Beijing, Atmos. Pollut. Res., 12, 230–241, https://doi.org/10.1016/j.apr.2020.12.010, 2021.

Zhang, D., He, B., Yuan, M., Yu, S., Yin, S., and Zhang, R.: Characteristics, sources and health risks assessment of VOCs in Zhengzhou, China during haze pollution season, J. Environ. Sci., 108, 44–57, https://doi.org/10.1016/j.jes.2021.01.035, 2021.

Zhang, D., Li, X., Yuan, M., Xu, Y., Xu, Q., Su, F., Wang, S., and Zhang, R.: Characteristics and sources of nonmethane volatile organic compounds (NMVOCs) and O_3–NO_x–NMVOC relationships in Zhengzhou, China, Atmos. Chem. Phys., 24, 8549–8567, https://doi.org/10.5194/acp-24-8549-2024, 2024.

Zhang, F., Shang, X., Chen, H., Xie, G., Fu, Y., Wu, D., Sun, W., Liu, P., Zhang, C., Mu, Y., Zeng, L., Wan, M., Wang, Y., Xiao, H., Wang, G., and Chen, J.: Significant impact of coal combustion on VOCs emissions in winter in a North China rural site, Sci. Total Environ., 720, 137617, https://doi.org/10.1016/j.scitotenv.2020.137617, 2020.

Zhang, J., Sun, Y., Wu, F., Sun, J., and Wang, Y.: The characteristics, seasonal variation and source apportionment of VOCs at Gongga Mountain, China, Atmos. Environ., 88, 297–305, https://doi.org/10.1016/j.atmosenv.2013.03.036, 2014.

Zhang, Z., Yan, X., Gao, F., Thai, P., Wang, H., Chen, D., Zhou, L., Gong, D., Li, Q., Morawska, L., and Wang, B.: Emission and health risk assessment of volatile organic compounds in various processes of a petroleum refinery in the Pearl River Delta, China, Environ. Pollut., 238, 452–461, https://doi.org/10.1016/j.envpol.2018.03.054, 2018.

Zheng, H., Kong, S., Xing, X., Mao, Y., Hu, T., Ding, Y., Li, G., Liu, D., Li, S., and Qi, S.: Monitoring of volatile organic compounds (VOCs) from an oil and gas station in northwest China for 1 year, Atmos. Chem. Phys., 18, 4567–4595, https://doi.org/10.5194/acp-18-4567-2018, 2018.

Zheng, J., Zhong, L., Wang, T., Louie, P. K. K., and Li, Z.: Ground-level ozone in the Pearl River Delta region: Analysis of data from a recently established regional air quality monitoring network, Atmos. Environ., 44, 814–823, https://doi.org/10.1016/j.atmosenv.2009.11.032, 2010.

Zhou, Z., Xiao, L., Fei, L., Yu, W., Lin M., Huang, T., Zhang, Z., and Tao J.: Characteristics and sources of VOCs during ozone pollution and non-pollution periods in summer in Dongguan industrial concentration area, Environm. Sci., 43, 4497–4505, https://doi.org/10.13227/j.hjkx.202111285, 2022.

Zou, Y., Yan, X. L., Flores, R. M., Zhang, L. Y., Yang, S. P., Fan, L. Y., Deng, T., Deng, X. J., and Ye, D. Q.: Source apportionment and ozone formation mechanism of VOCs considering photochemical loss in Guangzhou, China, Sci. Total Environ., 903, 166191, https://doi.org/10.1016/j.scitotenv.2023.166191, 2023.

Zuo, H., Jiang, Y., Yuan, J., Wang, Z., Zhang, P., Guo, C., Wang, Z., Chen, Y., Wen, Q., Wei, Y., and Li, X.: Pollution characteristics and source differences of VOCs before and after COVID-19 in Beijing, Sci. Total Environ., 907, 167694, https://doi.org/10.1016/j.scitotenv.2023.167694, 2024.